Structural characterization of Eu 2O 3–MgO–Na 2O–Al 2O 3–SiO 2 glasses with varying Eu 2O 3 content: Raman and NMR studies

ARTICLE *in* JOURNAL OF NON-CRYSTALLINE SOLIDS · JANUARY 2003

Impact Factor: 1.77 · DOI: 10.1016/S0022-3093(02)01594-6

Available online at www.sciencedirect.com
SCIENCE DIRECT®
Journal of Non-Crystalline Solids 315 (2003) 43–53
JOURNAL OF NON-CRYSTALLINE SOLIDS
www.elsevier.com/locate/jnoncrysol

Structural characterization of Eu_2O_3–MgO–Na_2O–Al_2O_3–SiO_2 glasses with varying Eu_2O_3 content: Raman and NMR studies

Zhandos N. Utegulov [a,*], Margaret A. Eastman [b], S. Prabakar [c], Karl T. Mueller [c], Abdulatif Y. Hamad [d], James P. Wicksted [a], George S. Dixon [a]

[a] *Department of Physics, Center for Lasers and Photonics Research, Oklahoma State University, Stillwater, OK 74078, USA*
[b] *Department of Chemistry, Oklahoma State University, Stillwater, OK 74078 USA*
[c] *Department of Chemistry, Pennsyvania State University, 152 Davey Laboratory, University Park, PA 16802, USA*
[d] *Department of Physics, Southern Illionois University, Edwardsville, IL 62026, USA*

Received 4 December 2000; received in revised form 16 April 2002

Abstract

Raman, ^{27}Al and ^{29}Si NMR spectroscopies are used to investigate the structure of $[0.15Na_2O–0.12MgO–0.03Al_2O_3–0.70SiO_2]_{(100-x)}$: $[Eu_2O_3]_x$ glasses with varying Eu_2O_3 content ($x = 0$, 0.73, 1.26, 3.90, 5.26 and 8.11 mol%). Spectral changes in the Raman envelope at (900–1240) cm^{-1} indicate that the number of silica tetrahedra with more than one non-bridging oxygen (NBO) per tetrahedron and the number of silica tetrahedra with one NBO associated with Eu increase with increasing rare-earth concentration. ^{29}Si MAS NMR spectra show a single broad peak with maxima at frequencies attributable to a predominance of Q^3 species. Quantitative ^{27}Al and ^{29}Si NMR spectroscopies show that aluminum and silicon species become less observable as Eu_2O_3 content increases, presumably due to interactions with paramagnetic europium. The ^{27}Al NMR spectra reveal the presence of only tetrahedrally coordinated Al sites, with a gradual increase in the structural disorder associated with these sites as the concentration of Eu_2O_3 increases. This is in agreement with the appearance of the broad Raman band at 790 cm^{-1} attributed to Al–O stretching vibrations with Al in fourfold coordination.

PACS: 42.70.Ce; 63.50.+x; 76.60.–k; 78.30.Ly

1. Introduction

Rare-earth doped glasses have attracted much attention for their potential use as optical storage materials [1]. Laser-induced permanent and transient refractive index gratings have been studied in Eu^{3+}-doped silicate glass [2–4]. The ability to create laser-induced gratings in these glasses is related to the production of high-energy phonon modes through non-radiative decay of excited Eu^{3+} ions in the glass network [2,4]. These phonons are associated with Si–NBO stretching vibrations. In addition, a recent study has indicated a significant increase in grating formation related to the existence of AlO_4^- tetrahedra [4]. Therefore, it is of

* Corresponding author. Tel.: +1-405 744 2821; fax: +1-405 744 6811.
E-mail address: uzhando@okstate.edu (Z.N. Utegulov).

0022-3093/03/$ - see front matter
PII: S0022-3093(02)01594-6

interest from both a fundamental as well as an applied viewpoint to study the underlying phonon physics and aluminum coordination in these glasses as the Eu^{3+} concentration is varied.

Rare-earth aluminosilicate glasses demonstrate unusual physical properties, e.g., high hardness [5] and large paramagnetic susceptibilities [6]. Rare-earth ions entering the aluminosilicate glass usually act as network modifiers, causing the formation of a wide distribution of silicon-non-bridging oxygens (Si–NBOs) [7–9]. Raman spectral studies indicate that the structure of rare-earth aluminosilicate glass is more disordered than that of alkali or alkaline earth aluminosilicate glasses due to the broader distribution of various types of SiO_4 tetrahedra present in the glass [9]. These structural units are commonly denoted Q^n, with n being the number of bridging oxygens per tetrahedron. Si–NBO vibrations with NBO coordinated to lanthanide lie at lower wave numbers in the Raman spectrum than those with NBO coordinated to ions of lower valency [10,11]. The high field strength of rare-earth ions has been proposed to be responsible for the reduced force constant of the Si–NBO bond with NBO coordinated to rare-earths [12].

^{29}Si MAS NMR spectra of alkali [13,14], alkaline earth [14,15], and yttrium [8] aluminosilicate glasses are poorly resolved and do not show distinct peaks for different Q^n species. However, some information has been derived from the position of the resonance, which may indicate which of the Q^n species is predominant (often Q^2, Q^3 or Q^4). Also informative are the shape and breadth of the resonance, which suggest the range and relative amounts of different Q^n species. ^{27}Al MAS NMR spectra of glasses have shown that the coordination of aluminum is usually fourfold in alkali aluminosilicate glass [13,16] and alkaline earth aluminosilicate glass [15]. Octahedrally coordinated Al has also been found in some rare-earth doped aluminosilicate glasses [8,17,18].

Earlier investigations of aluminosilicate glasses were limited to the structure of either glasses containing trivalent modifier ions [5,8,9,17–19] or glasses containing divalent and/or monovalent ions only [13,15,16,20]. The structure of Eu^{3+} doped soda magnesia alumina silica (EDSMAS) glass is expected to be more complicated than that of binary, ternary and quaternary glasses. In the present work, we use Raman and NMR spectroscopies to study the structure of aluminosilicate glasses containing trivalent modifier (Eu^{3+}) ions, divalent (Mg^{2+}), and monovalent (Na^+) ions. Using Raman scattering, we investigate the local structure of the glass by probing high-, mid- and low-frequency optical phonons. ^{27}Al and ^{29}Si MAS NMR spectroscopies are used to provide information about Al and Si coordination sites, respectively. The disappearance of the NMR signals with increasing Eu content is examined quantitatively for ^{27}Al and ^{29}Si.

2. Experimental

2.1. Sample preparation

EDSMAS glass compositions used in our study are given in Table 1. Glass samples were made in batches from sodium carbonate, magnesium earth carbonate, europium carbonate, alumina and silica precursor powders of 99.997%, 99.996%, 99.99%, 99.999% and 99.999% purity, respectively. Carbonate powders were utilized, whenever possible, to improve precursor subdivision in the final melt. All powders were mixed for approximately 1 h. The mix of powders was held at temperatures of 800 °C and then 1350 °C for 18 h each, then raised to 1650 °C, where it was maintained for 50 h. The melt was stirred twice using a platinum rod during this 50-h period. Finally, the temperature was lowered to 1550 °C at a rate of −50 °C/h. Once at

Table 1
Batched composition of EDSMAS glass samples

Sample ID	Eu_2O_3	MgO	Na_2O	SiO_2	Al_2O_3
E0	0.00	12.00	15.00	70.00	3.00
E0.73	0.73	11.91	14.89	69.49	2.98
E1.26	1.26	11.85	14.81	69.12	2.96
E3.90	3.90	11.53	14.42	67.27	2.88
E5.26	5.26	11.37	14.21	66.32	2.84
E8.11	8.11	11.03	13.78	64.32	2.76

All numbers are given in mol%. The estimated uncertainties in the glass batched compositions are ±0.03 mol% for each oxide component in the glass.

1550 °C, the glass was transferred to a 425 °C annealing furnace, where the temperature was raised to 725 °C and held for at least 1 h. The annealing furnace was then turned off, and the glass was allowed to cool to room temperature. Bubble free samples with high optical quality were made using this method.

2.2. Raman spectroscopy

Light of 457.9 nm wavelength from an Ar^+ laser was chosen since this is not at resonance with the Eu^{3+} ions, thus lowering the absorption and making the effect of fluorescence on the Raman spectrum negligible. [1] A 200-mW laser beam was directed into the parallelepiped-shaped transparent glass sample placed on a horizontal adjustable holder with the scattered light collected at right angles to the incident beam. Unpolarized Raman spectra were taken at a scan rate of 0.33 cm^{-1}/s using a double monochromator Raman spectrometer. At the laser wavelength of 457.9 nm and utilizing slit widths of 200 μm, the spectral resolution of the Raman spectrometer was 2.27 cm^{-1}.

2.3. NMR spectroscopy

^{27}Al and ^{29}Si NMR spectra were obtained at 7.07 T (78.434 MHz, 59.800 MHz) with a 5 mm triple-resonance magic-angle spinning (MAS) probe. ^{27}Al spectra were also obtained at 11.74 T (130.183 MHz) with a 2.5 mm MAS probe. Finely ground powder samples were packed in cylindrical zirconia rotors with plastic drive tip, spacer, and cap. Pulse widths used to calculate the radiofrequency field strengths at 7.07 T were measured for ^{27}Al on a liquid sample of 1 M aqueous $Al(NO_3)_3$ and for ^{29}Si on solid sodium-3-trimethylsilylpropionate. All experiments were performed at room temperature without temperature control.

Measurements of ^{27}Al spin relaxation time constants (T_1 and T_2) for the central transition were made at 78.434 MHz on samples spinning at 10.000 ± 0.005 kHz using the inversion recovery (π_s-τ-$(\pi/2)_s$-acquire) pulse sequence for T_1 and spin-echo ($(\pi/2)_s$-τ-π_s-τ-acquire) pulse sequence for T_2, where the subscript 's' signifies a solid-state pulse width. Following Haase et al. [21,22] a weak radiofrequency field strength (6.0 kHz) was used to selectively excite the central transition. The $(\pi/2)_s$ pulse width (14 μs) was 1/3 of the liquid-state $\pi/2$ pulse width, demonstrating selective excitation of the central transition [23]. A background ^{27}Al MAS spectrum of $Na_2C_2O_4$ for each value of τ (for both sequences) was obtained, and these spectra were subtracted from the corresponding spectra of the glasses. A delay of 1 s between scans was used, and 1200 scans were averaged for each τ value for ^{27}Al T_2 measurements. Synchronous sampling [24] was achieved by selecting τ values such that the entire length of the pulse sequence prior to acquisition corresponded to an even integral number of rotor periods. ^{27}Al T_1 measurements were made with a delay of 2 s between scans and 2000 scans averaged. Measurements of ^{29}Si T_2 utilized the spin-echo pulse sequence with synchronous sampling and a $\pi/2$ pulse width of 9 μs. Pulse delays depended upon the sample and are provided in Section 3.

To estimate the amount of aluminum in each glass sample detectable by NMR, quantitative ^{27}Al spectra were taken at 78.434 MHz without MAS by using a $\pi/24$ pulse width and field strength of 20.8 kHz. A similarly short pulse width has been recommended by Man et al. [23] for reliable quantitative analysis. Each of the glass samples and two standards, aluminum potassium sulfate ($AlK(SO_4)_2$–$12H_2O$) and aluminum acetyl acetonate, were weighed on a balance after packing into a rotor, and the mass of the rotor was subtracted to give the sample mass. The chemical formula was used to calculate the number of moles of Al in the experimentally determined mass. ^{27}Al spectra were obtained for each sample with 3600 scans averaged and a 2.0 s delay between acquisitions. As there is ^{27}Al background signal from both the probe and the rotor assembly, three background spectra were taken with the same parameters used for the quantitative spectra: one spectrum of the rotor packed with sodium oxalate ($Na_2C_2O_4$), and two spectra of the empty rotor. The entire series of

[1] We have shown elsewhere (see [3]) that weak excitation of Eu^{3+} ions still occurs due to phonon-assisted energy transfer and/or the breadth of the inhomogeneously broadened absorption band.

glass sample, standard, and background spectra were displayed on the same scale and the Al resonances were integrated. After subtraction of the average of the three background integrals from the standard integrals, the known (calculated) quantities of Al in the standards were used to obtain an average conversion factor of (mole Al)/(integral unit). The conversion factor was then used to obtain the number of moles of Al from the background-corrected integrals of the glass samples. This method depends upon the reasonable assumption that all of the ^{27}Al in the standards is detectable by ^{27}Al NMR.

3. Results

3.1. Raman spectroscopy

Unpolarized Raman spectra for the EDSMAS glasses with various Eu_2O_3 concentrations are shown in Fig. 1. The Raman peak intensities are a function of not only the number of vibrating modes but also bond polarizabilites, therefore only the relative changes in abundances of various Q^n species with varying Eu content can be deduced from changes in the Raman peak intensities. With the increase of the rare-earth content, the Raman envelope at (900–1240) cm^{-1} shifts toward lower wave numbers and the band at 970 cm^{-1} gradually merges with the band at 1100 cm^{-1}.

The Raman band at 575 cm^{-1} attributed to the bridging oxygen breathing mode in both pure silicate- [25] and (Si,Al)-three-membered rings [16,26], gradually shifts toward higher frequencies from 575 to 620 cm^{-1} with increasing Eu content of the glass. The band at 480 cm^{-1} is similarly attributed to the bridging oxygen breathing mode in both pure silicate- [25] and (Si,Al)-four-membered rings [27]. This peak shifts toward lower frequencies from 480 to 460 cm^{-1} with the increase of europium doping into the EDSMAS glass. The height of the 575 cm^{-1} Raman band increases with respect to the 480 cm^{-1} band. The peak at 790 cm^{-1} is assigned to the tetrahedral Si cage motions and to Al–O stretching vibrations of Al in tetrahedral coordination [16,28]. A low-frequency shoulder at ~240 cm^{-1} appears with the introduction of rare-earth ions. The Boson peak at ~85 cm^{-1} is also affected by the rare-earth ions and becomes especially pronounced at 8.1 mol% of Eu_2O_3.

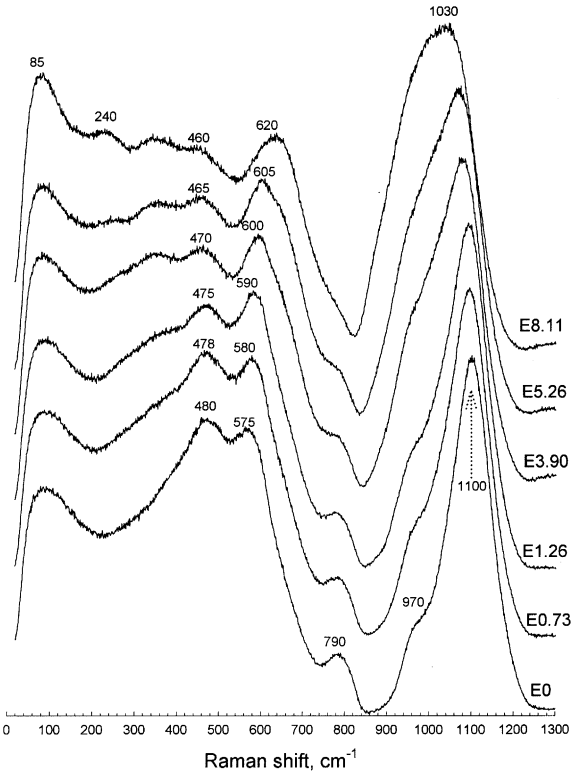

Fig. 1. Unpolarized Raman spectra of the EDSMAS glasses demonstrate changes in the structure with variation in mol% of Eu_2O_3.

3.2. NMR spectroscopy

Listed in Table 2 are the relaxation time constants for ^{27}Al with magic-angle spinning for four of the glass samples. Both T_1 and T_2 change very little with europium content. Table 3 presents the

Table 2
^{27}Al MAS NMR relaxation times

Sample ID	T_1 (ms)	T_2 (ms)
E0	25 ± 3	4.6 ± 0.1
E1.26	31 ± 3	4.7 ± 0.1
E3.90	26 ± 3	4.2 ± 0.1
E8.11	23 ± 2	3.9 ± 0.2

Fitting equations are $y = A_1(1 - A_2\exp(-\tau/T_1))$ for T_1 and $y = A_1\exp(-2\tau'/T_2)$ for T_2 where $\tau' = \tau + (1/2)(t_{\pi/2}) + (1/2)(t_\pi)$.

Table 3
Quantitative NMR analysis of ^{27}Al in glass samples

Sample	Mass (g)	Formula weight (g/mol)	Calculated mole Al (± 0.01) $\times 10^4$	Corrected integral	Expt. mole Al ($\times 10^4$)	Observable Al (%)
$AlK(SO_4)_2$–$12H_2O$	0.1559	474.4	3.29	0.715	–	–
AlAcAc	0.1000	324.3	3.08	0.659	–	–
EO	0.2035	6771.2	1.81	0.372	1.71 ± 0.09	94 ± 5
E0.73	0.2116	6978.9	1.81	0.365	1.68 ± 0.09	93 ± 5
E1.26	0.2121	7129.3	1.76	0.344	1.58 ± 0.09	90 ± 5
E3.90	0.2318	7879.9	1.69	0.257	1.18 ± 0.08	70 ± 5
E5.26	0.2704	8266.5	1.86	0.190	0.87 ± 0.07	47 ± 4
E8.11	0.2270	9076.8	1.38	0.090	0.41 ± 0.06	30 ± 4

Errors of 2% in integration, 0.5 mg in weighing, 0.03 mol% Al in glass composition, and 0.05 g/mol in molecular weight were propagated to give final errors in calculated and experimental moles of aluminum. Three background spectra (empty rotor or rotor + $Na_2C_2O_4$) had integrals of 0.493, 0.496, and 0.503; the average of these three values was subtracted from the integral to give the corrected integral.

results of the quantitative ^{27}Al spectroscopy. Despite the substantial error, it is clear that as the mol% of Eu_2O_3 in the glass increases, the percentage of the ^{27}Al calculated from the glass composition that can be detected by NMR decreases, going down to about 30% at 8.11 mol% of Eu_2O_3.

Fig. 2(a) shows how the observed ^{29}Si signal varies with pulse delay for two of the glass samples. For the E0 sample, a delay of over 3000 s is necessary to allow for complete relaxation, while for the E8.11 sample a delay of 45 s is adequate, suggesting that T_1 decreases substantially as Eu enters the glass. Fig. 2(b) demonstrates that the ^{29}Si MAS T_2 is shorter for the E8.11 sample than for the E0 sample. The ^{29}Si MAS spectra for these two samples in Fig. 2(c) shows a single broad peak at −93 to −95 ppm, which is broader in the sample with europium. The ratio of the integrals of the two spectra, after division by the number of scans and number of moles of ^{29}Si, is $6 \pm 2\%$.

Fig. 3 shows ^{27}Al MAS spectra of the glasses, which display a single peak at about 55 ppm that broadens as the mol% of Eu_2O_3 increases. Table 4 shows the peak positions and full widths at half maximum (FWHM) for the ^{27}Al spectra.

4. Discussion

With no europium present in the EDSMAS glass, the high-frequency portion of the Raman spectrum has two partially distinct bands at 970 and 1100 cm^{-1} attributable to Si–NBO stretching vibrations in Q^2 and Q^3 silicon tetrahedral groups, respectively [29]. The NBOs formed in E0 glass are due to Na^+ and Mg^{2+} cations, i.e. Q^3 and Q^2 species in this case are represented by Q^3-Mg, Q^3-Na and Q^2-Mg, Q^2-Na units. The shift toward lower wave numbers and change in the shape of the (900–1240) cm^{-1} band with increasing Eu_2O_3 content can be attributed to an increase in the Q^3-Eu species at about 1030 cm^{-1} [10] at the expense of Q^3-Na and Q^3-Mg species, as well as an increase in the contribution from Q^2 species and the development of contributions from Q^1 ($\sim$900 cm^{-1}) and Q^0 ($\sim$850 cm^{-1}) [29]. Thus, the net effect of the increase of the rare-earth ion content is the appearance and gradual increase of more depolymerized SiO_4 units in EDSMAS glass. We have estimated the fraction of all NBO atoms ($R_{\text{Total NBO}}$) and the fractions of NBOs associated with Na and Mg ($R_{\text{Na+Mg}}$) and with Eu ions (R_{Eu}). These values are shown in Table 5. In the estimation of the relative NBO amounts [30] it was assumed that Na^+, Mg^{2+} and Eu^{3+} ions in EDSMAS glass create one, two and three NBOs, respectively, and one Na^+ ion is needed to compensate the charge of one $[AlO_4]^-$ complex. Up to 5.26 mol% of Eu_2O_3, $R_{\text{Na+Mg}} > R_{\text{Eu}}$, but at 8.11 mol% of Eu_2O_3, R_{Eu} exceeds $R_{\text{Na+Mg}}$. Below 8.11 mol% of Eu_2O_3, the peak at $\sim$1100 cm^{-1} representing Q^3-Na and Q^3-Mg remains dominant, but at 8.11 mol% of Eu_2O_3 this peak shifts closer to the expected position of Q^3-Eu

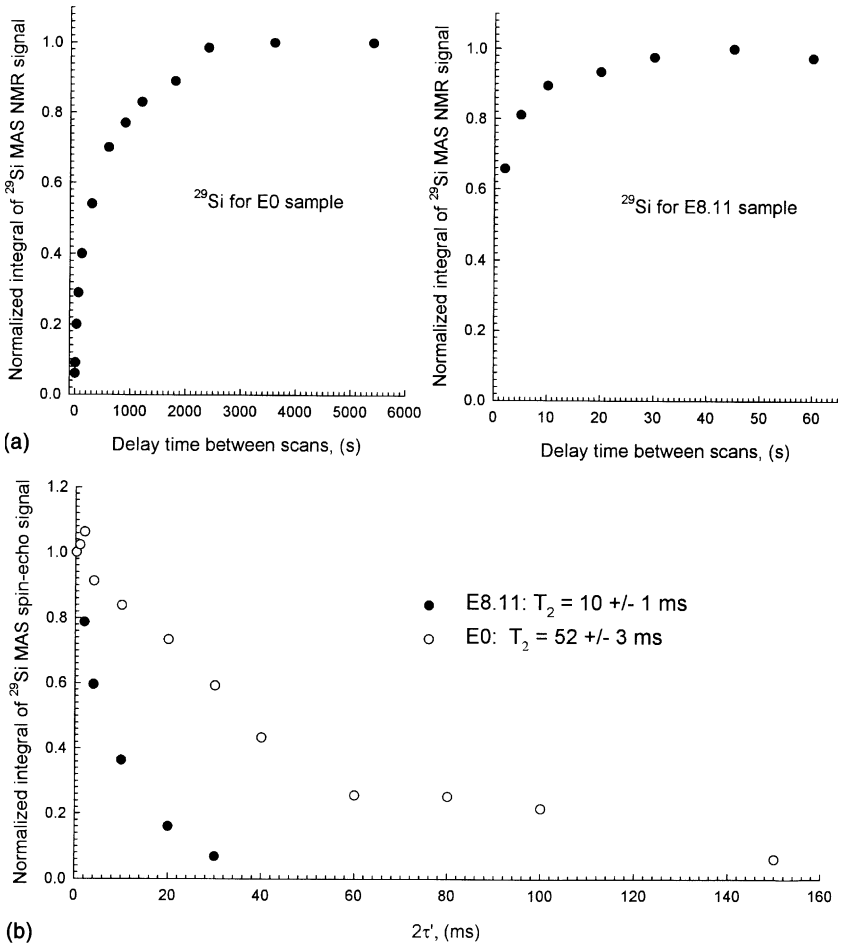

Fig. 2. (a) The integral of the signal from ^{29}Si MAS spectra vs. delay time between scans shows the different delays required to obtain quantitative spectra. Spectra were taken at 59.800 MHz with a spinning rate of 8.000 ± 0.005 kHz, and a $\pi/2$ pulse width of 9.0 μs. The number of scans averaged was 8 for 0 mol% Eu_2O_3 and 1800 for 8.11 mol% Eu_2O_3. (b) Spin-echo data provide T_2 measurements for the glasses with 0 mol% Eu_2O_3 (3600 s pulse delay, 8 scans averaged) and 8.11 mol% Eu_2O_3 (45 s pulse delay, 500 scans averaged) mol% Eu_2O_3. The parameter τ' is defined in the legend of Table 2, along with the equation used in fitting. (c) Shown are ^{29}Si MAS spectra taken at 59.800 MHz with a spinning rate of 8.000 ± 0.005 kHz, and a $\pi/2$ pulse width of 8.0 μs. Integrals of spectral intensity are 4.7 ± 0.5 for 0 mol% Eu_2O_3 (240.8 ± 0.5 mg sample weight, 3600 s pulse delay, 44 scans averaged) and 5.9 ± 0.6 for 8.11 mol% Eu_2O_3 (307.9 ± 0.5 mg sample weight, 45 s pulse delay, 1500 scans averaged). A line broadening of 100 Hz has been applied to the spectra. The peak positions and the FWHM were obtained by fitting Gaussian line shapes to the spectra.

at $\sim$1030 cm^{-1}. The trend in the estimated total ratio of NBOs vs. Eu_2O_3 content ($R_{\text{Total NBO}}$ in Table 5) also agrees with the increase in amplitude of the Raman spectra at 970 cm^{-1} and below, attributable to an increase in Q^n with $n \leqslant 2$. As the number of different Q^n species increases, the local structure of the EDSMAS glass becomes not only more depolymerized but also more disordered, which is in agreement with previous studies of rare-earth aluminosilicate glasses [8,9,18] and rare-earth alkaline silicate glasses [31]. This interpretation of the spectra is also in agreement with the contention of Brawer and White [32], who suggested that high field strength modifier ions lead to highly disordered structures, with a broad distribution in the types of SiO_4 tetrahedra.

The frequency increase of the Raman band at 575 cm^{-1} assigned to the bridging oxygen breath-

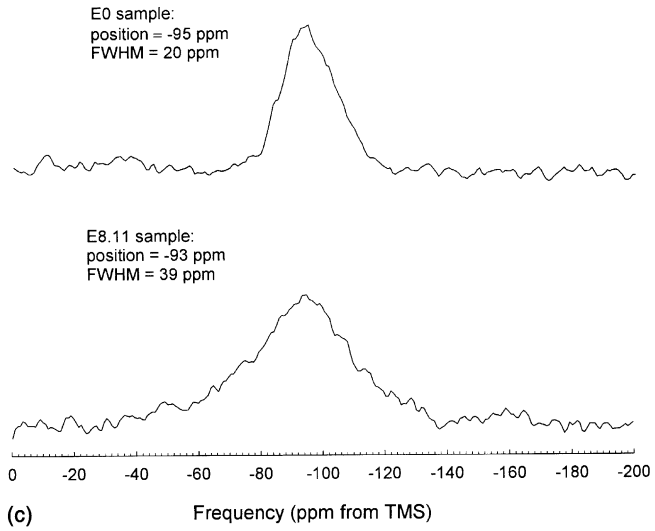

Fig. 2 (*continued*)

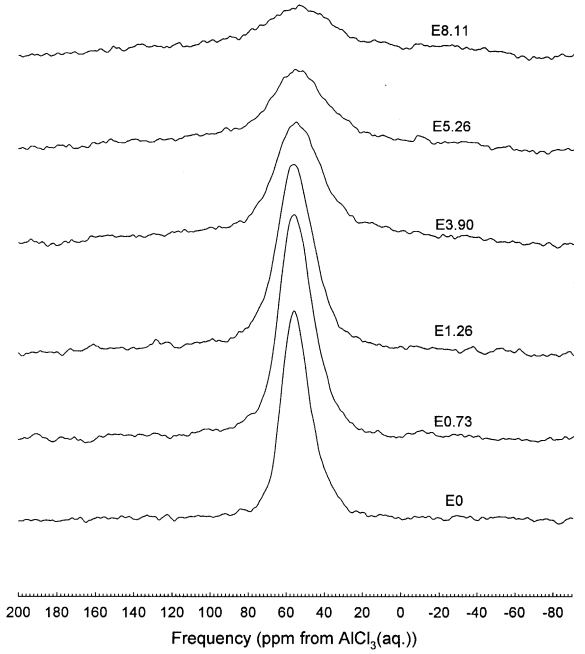

Fig. 3. ^{27}Al MAS spectra were obtained at 130.183 MHz with a spinning rate of 16.000 ± 0.005 kHz, and a $\pi/20$ pulse width of 1.0 μs corresponding to a radiofrequency field strength of 25 kHz. The delay between scans was 5 s and the number of scans averaged was 1024. The rotor and probe did not have significant ^{27}Al background signal.

Table 4
Peak positions and FWHMs in the ^{27}Al MAS NMR spectra to EDSMAS glasses

Sample ID	^{27}Al peak position (ppm)	^{27}Al FWHM (ppm)
E0	55	19
E0.73	55	23
E1.26	56	25
E3.90	54	34
E5.26	54	42
E8.11	55	55

The results were obtained by fitting Gaussian line shapes to the spectra. The error is ±1 ppm.

Table 5
Estimated relative ratios of NBOs (R_{Na+Mg} and R_{Eu}) in the glass due to ($Na^+ + Mg^{2+}$) and Eu^{3+} ions, respectively

Sample ID	R_{Na+Mg}	R_{Eu}	$R_{Total\ NBO}$
E0	0.273	0	0.273
E0.73	0.269	0.025	0.294
E1.26	0.267	0.043	0.310
E3.90	0.255	0.130	0.385
E5.26	0.249	0.173	0.422
E8.11	0.237	0.262	0.499

The ratio of the total number of NBOs to the total number of oxygens is denoted by $R_{Total\ NBO}$.

ing mode in the three-membered rings with increasing Eu^{3+} resembles the one reported by Krol and Smets [12] with the increase of high field strength ions ($T1^+$, In^{3+}, Sc^{3+}, Y^{3+} and La^{3+}) in sodium silicate glass. Since Eu^{3+} ions have larger ionic radii then Na^+ and Mg^{2+} ions, the relative

increase of Eu^{3+} concentration with respect to the concentrations of Na^{+} and Mg^{2+} ions leads to an increase in the formation of three-membered rings, as a result of the formation of larger cages in the glass structure [16], explaining the increase of the height of the 575 cm^{-1} Raman band.

The low-frequency Raman spectrum exhibits a shoulder at around 240 cm^{-1}, which can be reasonably attributed to modes involving Eu–O vibrations, since Eu ions form much weaker bonds with oxygen and the mass of Eu is much higher than that of Si or Al. This Raman shift is consistent with that of Sm–O vibrations in samarium aluminosilicate glass [9] and various rare-earths in phosphate glasses [33]. From fluorescence spectroscopic studies, the presence of different structural sites occupied by europium ions was deduced for the EDSMAS glasses [3] and for the europium lithium calcium aluminosilicate glasses [34], which might explain the broadness of the 240 cm^{-1} band.

The height of the Boson peak at ~85 cm^{-1} gradually increases with respect to the band at 480 cm^{-1} band. It has been proposed that the polarizability and atomic mass of rare-earth ions, as well as the ionicity of their chemical bonding, are the origin of the Boson band amplitude enhancement with the increase of the rare-earth (Pr^{3+}, Dy^{3+}, Nd^{3+}, Ce^{3+}) concentration [35]. Our recent Brillouin studies also indicate that the overall bonding in the EDSMAS glass becomes more ionic with the increase of Eu_2O_3 content [36].

Quantitative analysis of ^{27}Al by NMR has shown that as Eu content increases, the percentage of ^{27}Al that can be observed by NMR decreases. Fig. 4 demonstrates the close resemblance of our data to a model in which one quarter of all Eu ions, presumably in the form of Eu^{3+}, contacts ^{27}Al closely enough to broaden the resonance by paramagnetic enhancement of relaxation to the extent that it is not observable. The experimental points below 3.90 mol% of Eu_2O_3 are also well fit by the assumption that 1/5 of all Eu contacts Al (not shown). Although the fraction of Eu in close proximity to aluminum may not be accurately determined by this analysis, the model in which every Eu is near Al is clearly inappropriate.

Although we have not presented quantitative ^{29}Si NMR data for the complete set of glasses,

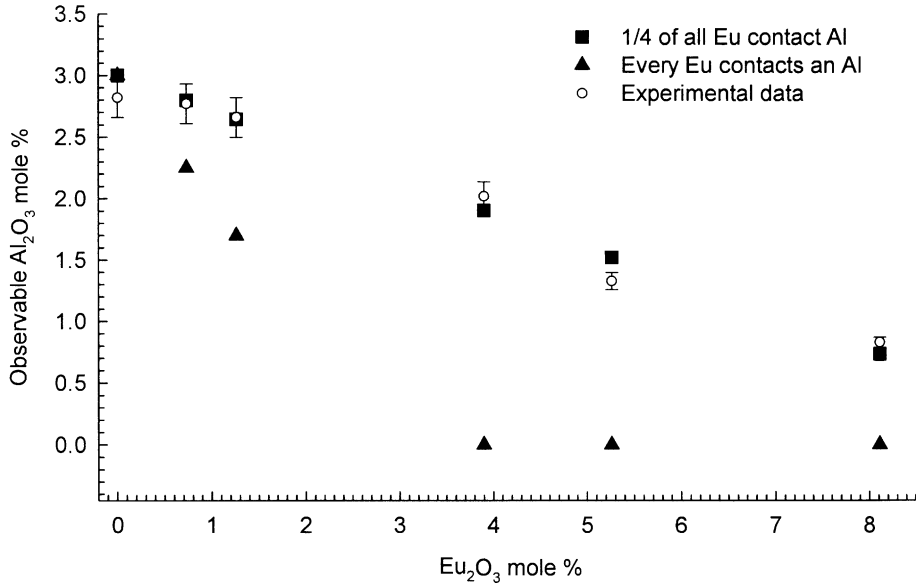

Fig. 4. Experimental data for the mol% Al_2O_3 observable by NMR as a function of mol% Eu_2O_3 in the glass are compared to calculations based on short range contact interactions between europium and aluminum. Calculated data assume that any Al in close contact with Eu will not be observable. Experimental data were obtained by calculating the percentage of invisible Al from Table 3 and subtracting the corresponding percentage of Al_2O_3 from the mol% Al_2O_3 in the glass (Table 1).

because of the long time required to obtain such data due to the long T_1 relaxation times, loss of ^{29}Si signal with increasing europium concentration is evident. In the spectra of Fig. 2(c) the E8.11 sample shows a signal-to-noise ratio comparable to that of the E0 sample with a much larger number of scans averaged, indicating overall poorer signal-to-noise. Weighing of the samples permitted the integrals of the two spectra to be divided by number of moles of ^{29}Si and number of scans averaged. Assuming that all ^{29}Si is observable in the E0 sample, the ratio of these integrals shows that 6% of the ^{29}Si is observable in the E8.11 sample, suggesting that the signal loss for ^{29}Si is greater than for ^{27}Al.

The single peak in the ^{27}Al MAS spectra can be assigned to aluminum coordinated with four oxygens, since the resonance frequency is similar to that seen for AlO_4 in lanthanum and yttrium aluminosilicate glasses [18]. The coordination of aluminum is generally fourfold in alkali aluminosilicate glass [13,16] and alkaline earth aluminosilicate glass [15]. Both fourfold and sixfold coordination of aluminum have been observed in rare-earth (La, Ce, Eu) aluminosilicate glasses [17,18,37] and yttrium aluminosilicate glass [8,18]. In comparing these observations to our detection of only Al(4) in the EDSMAS glasses, it may be important to consider that our concentrations of europium are below the rare-earth or yttrium concentrations that yielded sixfold coordination (10–40 mol% of rare-earth or yttrium oxide). In addition, the overall concentration of aluminum is much higher (10–40 mol% Al_2O_3) in the above mentioned glass systems compared to Al content in the EDSMAS glasses. Al(6) sites may not form until a certain level of rare-earth and Al content is reached. Small spectral features in the region of the spectrum usually assigned to octahedral Al species do increase with Eu content (Fig. 3). However, these features are not much above the noise level.

The ^{27}Al MAS T_2 values suggest homogeneous line widths of 0.9–1.0 ppm, for the E0 sample and those containing Eu_2O_3. Since ^{27}Al MAS line widths (about 19–55 ppm) are much larger than this, the line widths of the glasses are probably the result of a dispersion of chemical shifts and/or second-order quadrupolar shifts due to a variety of local structures around the Al(4), as might be expected for a glass. Considering that T_2 decreases only a small amount with Eu content, the observed broadening of the Al(4) resonances in the MAS spectrum as Eu content increases must be mainly due to increased disorder of the structure in the vicinity of aluminum, rather than enhanced relaxation by the paramagnetic Eu^{3+} ion. This is in agreement with the disordering of Al(4) sites that can be deduced from the broadening of the Raman band at 790 cm^{-1}.

As for ^{27}Al, the width of the ^{29}Si MAS peak cannot be accounted for by T_2 relaxation alone, since the T_2 values imply 0.1 and 0.5 ppm homogeneous widths for 0 and 8.11 mol% Eu_2O_3, respectively, while the actual widths are 20 and 39 ppm. Since, in contrast to the case for ^{27}Al, T_2 decreases substantially with an increase of the mol% of Eu_2O_3, the broadening of the ^{29}Si peak with increasing Eu concentration may be due at least in part to enhanced relaxation by the paramagnetic Eu^{3+} ion. An increase in structural disorder, such as a greater variety of bond lengths and bond angles, could also contribute to the line broadening. The situation is more complicated than for ^{27}Al, because the ^{29}Si MAS peak comprises a group of unresolved peaks representing Q^n units with a series of values of n, each of which has a dispersion of chemical shifts due to structural disorder. Hence, both the width and position of this composite peak could change with the relative amounts of the different Q^n species. Because the ^{29}Si line broadening could originate from a few different sources, it is difficult to make a conclusion regarding its relationship to structure.

Established ^{29}Si NMR resonance assignments for a variety of silicate and aluminosilicate glasses with alkali and alkaline earth modifiers are −76 to −88 ppm for Q^2, −85 to −97 ppm for Q^3, and −100 to −116 ppm for Q^4 [11,13,14,38–40]. Q^n(1Al) species are probably present in our glasses in small amounts because the Al_2O_3 concentration is low; the resonances for these species are at less negative frequency in comparison to those for the corresponding Q^n(0Al) species. Q^3 species are most prominent in both of the EDSMAS glass samples examined. The conclusion from the Raman spectra

that Q^n species with n equal to 2 or less are more prevalent as the mol% of Eu_2O_3 increases is not well supported by the ^{29}Si NMR spectra. However, the NMR results only monitor the observable subset of nuclei that are not too close to Eu^{3+}. It is probable that no shift in the position of the ^{29}Si peak is observed with europium content because there is a preferential disappearance of Q^n species with low n, which with their higher charge would have a greater propensity to coordinate with Eu^{3+}.

5. Conclusion

The structure of glasses of the formula $[0.15Na_2O–0.12MgO–0.03Al_2O_3–0.70SiO_2]_{(100-x)}$: $[Eu_2O_3]_x$ with varying Eu_2O_3 content ($x = 0$, 0.73, 1.26, 3.90, 5.26 and 8.11 mol%) has been studied with Raman and ^{27}Al and ^{29}Si NMR spectroscopies. Increase of the Eu_2O_3 content coincides with the formation of a broader distribution of NBOs. Raman spectra show that the concentration of silicon–oxygen tetrahedra containing a larger number of NBOs is found to increase gradually with increasing europium ion content, meaning that the glass becomes more depolymerized and disordered. SiO_4 units containing one NBO coordinated to europium ion become more prevalent relative to other species as the Eu_2O_3 concentration increases. The frequency downshift of the high-energy Raman envelope with the increase of Eu_2O_3 content can be understood as the height enhancement of the Q^n bands due to Si–NBO stretching bonds with $n \leqslant 2$. ^{29}Si MAS NMR spectra have an unresolved peak that most likely represents several Q^n species with predominance of Q^3, but the increase in depolymerization is not readily seen in the NMR, probably because of effects of paramagnetic Eu^{3+}.

^{27}Al NMR spectra show that Al is tetrahedrally coordinated in these glasses. Broadening of the ^{27}Al MAS NMR spectra, as well as broadening of the Al–O stretching band in the Raman spectra indicate an increase in the structural disorder around Al sites with increasing europium content.

Signal is lost with increasing content of Eu_2O_3 in both ^{27}Al and ^{29}Si NMR spectra, presumably due to rapid relaxation by paramagnetic Eu^{3+}. The reduction of observable ^{27}Al has been quantified and amounts to loss of 70% of the signal at 8.11 mol% of Eu_2O_3. Assuming observation of all ^{29}Si in the sample with 0 mol% of Eu_2O_3, 94% of the ^{29}Si signal is lost at 8.11 mol% of Eu_2O_3.

Acknowledgements

The authors thank Dr Joel Martin and Mr Charles Hunt for preparing some of the glass samples. This work was supported in part by the US Army Research Office under Grant # DA-AHO4-96-1-0322 and the National Science Foundation under Grant # DMP9705284. Funds for the Oklahoma Statewide Shared NMR Facility were provided by the National Science Foundation (BIR-9512269), the Oklahoma State Regents for Higher Education, the W.M. Keck Foundation and Conoco Inc. K.T.M is supported by a Camille Dreyfus Teacher-Scholar Award. The 500 MHz spectrometer at Penn State University was acquired with support from the National Science Foundation (CHE-9601572).

References

[1] E.G. Behrens, R.C. Powell, D.H. Backburn, Appl. Opt. 29 (11) (1990) 1619.
[2] E.G. Behrens, F.M. Durville, R.C. Powell, Phys. Rev. B 39 (9) (1989) 6076.
[3] A.Y. Hamad, J.P. Wicksted, G.S. Dixon, Opt. Mater. 12 (1999) 41.
[4] A.Y. Hamad, J.P. Wicksted, M.R. Hogsed, J.J. Martin, C.A. Hunt, G.S. Dixon, Phys. Rev. B 65 (2002) 064204.
[5] S. Tanabe, K. Hirao, N. Soga, J. Am. Ceram. Soc. 75 (3) (1992) 503.
[6] J.T. Kohli, I.E. Shelby, Phys. Chem. Glasses 32 (3) (1991) 109.
[7] J.E. Shelby, S.M. Minton, C.E. Lord, M.R. Tuzzolo, Phys. Chem. Glasses 33 (1992) 93.
[8] J.T. Kohli, J.E. Shelby, J.S. Frye, Phys. Chem. Glasses 33 (3) (1992) 73.
[9] J.T. Kohli, R.A. Condrate Sr., J.E. Shelby, Phys. Chem. Glasses 34 (3) (1993) 81.
[10] A.J.G. Ellison, P.C. Hess, J. Geophys. Res. 95 (B10) (1990) 15717.
[11] T. Schaller, J.F. Stebbins, M.C. Wilding, J. Non-Cryst. Soilds 243 (1999) 146.
[12] D.M. Krol, B.M.J. Smets, Phys. Chem. Glasses 25 (5) (1984) 119.

[13] S. Prabakar, K.J. Rao, C.N. Rao, Eur. J. Solid State Inorg. Chem. 29 (1992) 95.
[14] J. Murdock, J. Stebbins, Am. Mineral. 70 (1985) 332.
[15] C.I. Merzbacher, B.L. Sherriff, J.S. Hartman, W.B. White, J. Non-Cryst. Solids 124 (1990) 194.
[16] P.F. McMillan, A. Grzechnik, H. Chotalla, J. Non-Cryst. Solids 226 (1998) 239.
[17] S.-L. Lin, C.-S. Hwang, J. Non-Cryst. Solids 202 (1996) 61.
[18] T. Schaller, J.F. Stebbins, J. Phys. Chem. B 102 (1998) 10690.
[19] N.J. Clayden, S. Esposito, A. Aronne, P. Pernice, J. Non-Cryst. Solids 258 (1999) 11.
[20] A. Klonkowski, Phys. Chem. Glasses 24 (6) (1983) 166.
[21] J. Haase, K.D. Park, K. Guo, H.K.C. Timken, E. Oldfield, J. Phys. Chem. 95 (1991) 6996.
[22] J. Haase, E. Oldfield, J. Mag. Reson. A 101 (1993) 30.
[23] P.P. Man, J. Kilnkowski, A. Trokiner, H. Zanni, P. Papon, Chem. Phys. Lett. 151 (1988) 143.
[24] K.D. Schmitt, J. Haase, E. Oldfield, Zeolites 14 (1994) 89.
[25] R.A. Barrio, F.L. Galeener, E. Martinez, R.J. Elliott, Phys. Rev. B 48 (21) (1993) 15672.
[26] J.D. Kubicki, D. Sykes, Phys. Chem. Mine. 19 (1993) 381.
[27] D. Sykes, J.D. Kubicki, Am. Mineral. 81 (1996) 265.
[28] Ph. Colomban, J. Mater. Sci. 24 (1989) 3002.
[29] P.P. McMillan, Am. Mineral. 69 (1984) 622.
[30] A.K. Varshneya, in: Fundamentals of Inorganic Glasses, Academic Press, 1994, p. 99.
[31] H. Kozuka, Y. Li, K. Fukumi, S. Sakka, J. Mater. Sci. Lett. 6 (1987) 267.
[32] S.A Brawer, W.B. White, J. Chem. Phys. 63 (6) (1975) 2421.
[33] K. Sun, W.M. Risen, Solid State Commun. 60 (1986) 697.
[34] F. Durville, G.S. Dixon, R.C. Powell, J. Lumin. 36 (1987) 221.
[35] V.K. Tikhomirov, A. Jha, A. Perakis, E. Sarantopoulou, M. Naftaly, V. Krasteva, R. Li, A.B. Seddon, J. Non-Cryst. Solids 256&257 (1999) 89.
[36] G.Q. Shen, Z.N. Utegulov, S.M. Mian, J.P. Wicksted, Phys. Chem. Glasses 43 (2) (2002) 73.
[37] S. Tanabe, N. Soga, K. Hirao, T. Hanada, J. Am. Ceram. Soc 73 (1990) 1733.
[38] K. Glock, O. Hirsch, P. Rehak, B. Thomas, C. Jager, J. Non-Cryst. Solids 234 (1998) 113.
[39] J. Mahler, A. Sebald, Solid State Nucl. Reson. 5 (1995) 63.
[40] T. Maekaua, K. Kawamura, T. Yokokawa, J. Non-Cryst. Solids 127 (1991) 53.